

Detection, Identification, and Reconstruction of Faulty Sensors with Maximized Sensitivity

S. Joe Qin and Weihua Li

Dept. of Chemical Engineering, University of Texas, Austin, TX 78712

A new method proposed here detects, reconstructs, and identifies faulty sensors using a normal process model, which can be built from first principles or statistical methods such as partial least squares or principal component analysis. The model residual is used to detect sensor faults that demonstrate a deviation from the normal process model. To identify which sensor is faulty, a structured residual approach with maximized sensitivity is proposed to make one residual insensitive to one subset of faults but most sensitive to other faults. The structured residuals are subject to exponentially weighted moving average filtering to reduce the effect of noise and dynamic transients. The confidence limits for these filtered structured residuals are determined using statistical inferential techniques. In addition, other indices including generalized likelihood ratio test, cumulative sum, and cumulative variance of the structured residuals are compared to identify faulty sensors. The fault magnitude is then estimated based on the model and faulty data. Four types of sensor faults, including bias, precision degradation, drifting and complete failure, are simulated to test this method. Data from an industrial boiler process are used to test its effectiveness. Both single faults and simultaneous double faults are detected and uniquely identified with the method.

Introduction

Sensor validation is a necessary step in applying inferential sensors, model predictive control (MPC), and optimization to industrial processes. In a typical MPC application, for example, steady-state optimization is performed to find the optimal target values for the controlled variables and manipulated variances. If the sensors are faulty, the optimized target values are not valid. Therefore, an effective validation approach to detecting and identifying faulty sensors on-line is required. Once a faulty sensor is identified, it is desirable to estimate the fault magnitude and replace it with the best reconstruction in order to maintain the control system on-line even though a sensor has failed. We refer to the tasks of sensor fault detection, identification, and reconstruction as sensor validation.

Existing work in the area of sensor validation includes the use of neural networks (Kramer, 1991; Keeler and Ferguson,

1996), and the use of principal component analysis (PCA) to build the process model (Dunia et al., 1996). Once a normal model is built, Kramer (1991) uses an auto-associative neural network to estimate the replacement of the faulty sensors. However, this method does not completely eliminate the effect of the faulty sensors in estimating the replacement, resulting in a suboptimal solution. Dunia et al. (1996) propose the use of squared prediction error (SPE) to detect a sensor fault, the use of an optimization approach to reconstruct the fault, and identification of the faulty sensor by reconstructing each sensor in turn. This method relies on the use of PCA or partial least squares (PLS) to build the process model.

Early work related to sensor validation falls into two categories: gross error detection in data reconciliation and sensor fault detection, for example, for nuclear power plants and airplanes. The work in gross detection is reviewed thoroughly in Crowe (1996). Mah et al. (1976), Stanley and Mah (1977, 1981), and Romagnoli and Stephanopoulos (1981) are among the early work in gross error detection and rectification in

Correspondence concerning this article should be addressed to S. J. Qin.

chemical processes. Crowe et al. (1983) propose matrix projection approach to eliminate unmeasured variables present in the balance equations. Rollins and Davis (1992) propose an unbiased estimation technique (UBET) for the unbiased estimation of fault magnitudes. More recent work provides advances in the use of dynamic models, nonlinear models, neural networks, and additional statistical tests for the purpose of gross error detection (Crowe, 1996). The work by Tong and Crowe (1995) is among the first to apply PCA to analysis of the model residuals. Relations between several principal component tests and other traditional tests are also given. Dynamic gross error detection is studied by a number of researchers (Albuquerque and Biegler, 1996; Karjala and Himmelblau, 1996; Liebman et al., 1992). The use of auto-associative neural networks for sensor fault detection, identification, and reconstruction is proposed in Kramer (1991). Fantoni and Mazzola (1994) applied the work of Kramer (1991) to the sensor validation of nuclear power plants. In these methods, quasi-steady-state models are used to detect sensor gross errors. In the fault detection literature, Deckert et al. (1977) apply redundant hardware sensors to detect and identify abnormal sensors in an F-8 airplane. Model based fault detection and isolation techniques surveyed by Gertler (1988) can also be applied to the sensor validation problem.

In this work, we propose a new method that extends the work of Gertler and Singer (1985, 1990) for the detection and identification of faulty sensors using a normal, quasi-steady-state process model. The normal process model can be built from first principles or data using statistical methods such as PLS or PCA. The model *residual* is used to detect sensor faults. To identify which sensor is faulty, a *structured residual approach* with *maximized sensitivity* (SRAMS) is proposed to make one residual insensitive to one subset of faults but *most* sensitive to the other faults. Maximum isolation of sensor faults is achieved as a consequence.

To reduce false alarms due to dynamic transients, an EWMA filter is applied to the structured residuals. The confidence limits for these filtered structured residuals (FSR) are determined using statistical inferential techniques. By comparing the FSR with their respective confidence limits, faulty sensors can be identified. In addition, other indices including generalized likelihood ratio (GLR) test, cumulative sum (Qsum) and cumulative variance (Vsum) of the structured residuals are compared for the identification of faulty sensors. The best estimates for the faulty sensor and the fault magnitude are then derived based on the model and faulty data. Four types of sensor faults, including bias, precision degradation, drifting, and complete failure, are simulated to test the proposed method. Data from an industrial boiler process are used to test the effectiveness of the proposed methods.

Fault Detection

In this section, the fault detection task is performed under the assumption that the process is operating under quasi-steady-state conditions. In other words, the mass or energy accumulation rates in any part of the process are negligible comparing to the inlet and outlet energy or mass-flow rates. This assumption is reasonable for process operations that

avoid dramatic transients. When such a dynamic transient occurs, the steady-state conservation can be temporarily broken. EWMA filters will be applied to reduce the effect of dynamic transients. For processes that are constantly going through dynamic transients, a fully dynamic model should be used.

Model and fault representation

A normal process model can be represented in the following equation

$$Bx^*(t) = e^*(t) \quad (1)$$

where $x^* \in \mathbb{R}^n$ is a vector of normal sensor values, $B \in \mathbb{R}^{m \times n}$ is the model matrix, and $e^* \in \mathbb{R}^m$ is the model residual which contains measurement noise, process noise, and model errors. The matrix B can be derived from mass balance or energy balance of the process, or it can be generated from process data using statistical methods such as PCA and PLS. Under normal conditions, the model residual e^* can be assumed to be zero mean Gaussian noise. When a sensor fault occurs, the sensor measurement will contain the normal values of the process variables and the fault, that is,

$$x(t) = x^*(t) + \Xi_i f_i(t) \quad (2)$$

where $f_i(t) \in \mathbb{R}^{l_i}$ is a vector of the fault magnitude, $\Xi_i \in \mathbb{R}^{n \times l_i}$ is a matrix of fault directions, and l_i is the dimension of the fault. To represent a single sensor fault in the i th sensor, we choose $\Xi_i = [0 \ 0 \ \dots \ 1 \ \dots \ 0]^T$, which is the i th column of the identity matrix. To represent simultaneous multiple sensor faults, Ξ_i simply contains the corresponding columns of the identity matrix. Using the fault representation of Eq. 2 with a sensor fault, the model residual can be written as follows

$$e(t) = Bx(t) = Bx^*(t) + B\Xi_i f_i(t) = e^*(t) + B\Xi_i f_i(t) \quad (3)$$

A fault will in general cause the residual $e(t)$ to increase. The magnitude of the residual will be used to detect sensor faults. Since each sensor fault is represented by a distinct vector or matrix Ξ_i , fault identification can be accomplished by using the direction vectors.

Detection of sensor faults

The fault detection index is defined as follows

$$d = e^T(t) R_e^{-1} e(t) \quad (4)$$

where $R_e \equiv E\{e^*(t) e^{*T}(t)\}$ is the covariance matrix. When no fault is present, the fault detection index follows a Chi-square distribution (Romagnoli and Stephanopoulos, 1981)

$$d = e^{*T}(t) R_e^{-1} e^*(t) \sim \chi^2(m) \quad (5)$$

It is important to note that this fault detection index does not impose any probability assumption on the process vari-

ables $\mathbf{x}^*(t)$. Rather, it requires the residual $\mathbf{e}^*(t)$ to be zero-mean Gaussian white noise. As a result, the confidence limit for d is

$$d_\alpha = \chi_\alpha^2(m) \quad (6)$$

where α is the confidence level.

To reduce the effect of transients and noise in measured data, and EWMA filter is usually applied to the model residual,

$$\bar{\mathbf{e}}(t) = \gamma \bar{\mathbf{e}}(t-1) + (1-\gamma) \mathbf{e}(t) \quad (7)$$

where $0 \leq \gamma < 1$. It directly follows that under normal conditions

$$\bar{\mathbf{d}} = \bar{\mathbf{e}}^T(t) \bar{\mathbf{R}}_e^{-1} \bar{\mathbf{e}}(t) \sim \chi^2(m) \quad (8)$$

where $\bar{\mathbf{R}}_e = E\{\bar{\mathbf{e}}^*(t) \bar{\mathbf{e}}^{*T}(t)\}$. The filter index \bar{d} is preferred to the unfiltered index d in reducing false alarms due to noise, but it may introduce a delay in detecting faults.

If the normal process model is derived from process data using PCA or PLS, the sensor values $\mathbf{x}^*(t) \in \mathbb{R}^n$ is decomposed into

$$\mathbf{x}^*(t) = \mathbf{P}\mathbf{t} + \tilde{\mathbf{P}}\tilde{\mathbf{t}} \quad (9)$$

where $\mathbf{P} \in \mathbb{R}^{n \times (n-m)}$ are orthogonal eigenvectors associated with the principal eigenvalues $\lambda_1 \geq \lambda_2 \geq \dots \geq \lambda_{n-m}$ of the correlation matrix of $\mathbf{x}^*(t)$, and $\tilde{\mathbf{P}}$ are the remaining eigenvectors associated with the minor eigenvalues $\lambda_{n-m+1} \dots \lambda_n$. The vectors \mathbf{t} and $\tilde{\mathbf{t}}$ are the principal components and residual components, respectively. When m is chosen to be the number of equality constraints on the measurement vector $\mathbf{x}^*(t)$, the residual components $\tilde{\mathbf{t}}$ should contain random noise only. Since \mathbf{P} and $\tilde{\mathbf{P}}$ are mutually orthogonal, premultiplying Eq. 9 by $\tilde{\mathbf{P}}^T$ leads to

$$\tilde{\mathbf{P}}^T \mathbf{x}^*(t) = \tilde{\mathbf{P}}^T \mathbf{P} \mathbf{t} + \tilde{\mathbf{P}}^T \tilde{\mathbf{P}} \tilde{\mathbf{t}} = \tilde{\mathbf{t}} \quad (10)$$

In this case, the model residual $\mathbf{e}^*(t)$ corresponds to the residual components $\tilde{\mathbf{t}}$ and (Gertler et al., 1999)

$$\mathbf{B} = \tilde{\mathbf{P}}^T \quad (11)$$

In the context of PCA, it is conventional to use the squared prediction error (SPE) as a fault detection index

$$\text{SPE} = \mathbf{x}^T(t) \tilde{\mathbf{P}} \tilde{\mathbf{P}}^T \mathbf{x}(t) \leq \delta_\alpha^2 \quad (12)$$

The detection threshold for SPE can be determined as follows using an approximation distribution for SPE (Jackson and Mudholkar, 1979)

$$\delta_\alpha^2 = \theta_1 \left[\frac{c_\alpha \sqrt{2\theta_2 h_0^2}}{\theta_1} + 1 + \frac{\theta_2 h_0 (h_0 - 1)}{\theta_1^2} \right]^{1/h_0} \quad (13)$$

where $\theta_i = \sum_{j=l+1}^n \lambda_j^i$ for $i = 1, 2, 3$, $h_0 = 1 - 2\theta_1\theta_3/3\theta_2^2$, l is the number of principal components (PCs), and c_α is the confidence limit for the $1 - \alpha$ percentile in a Gaussian distribution.

It should be noted that the SPE confidence limit is derived under the following conditions:

- The process data \mathbf{x} is assumed to have normal distribution;
- An approximation is made for the SPE limit; and
- There is no specific requirement on the number of principal components.

The first two items appear to be shortcomings of the SPE detection index. These shortcomings can be avoided if one selects the number of principal components $l = n - m$ and uses d as the detection index.

Structured Residuals with Maximized Sensitivity Single sensor faults

After the detection index triggers an alarm, the faulty sensor(s) must be identified subsequently. There are many ways to identify the faulty sensors. Existing work in this area includes contribution plots (Miller et al., 1993), identification via sensor reconstruction (Dunia et al., 1996; Qin et al., 1997) and structured residuals (Gertler and Singer, 1985, 1990). In this section, we propose a new identification method called *structured residual approach with maximized sensitivity* (SRAMS). Then, we compare the SRAMS method with the conventional structured residual method.

For the case of single sensor fault in the i th sensor, Eq. 3 becomes

$$\mathbf{e}(t) = \mathbf{e}^*(t) = \mathbf{b}_i f_i(t) \quad (14)$$

where \mathbf{b}_i is the i th column of matrix \mathbf{B} . A set of structured residuals $\mathbf{r}(t)$ can be generated by pre-multiplying the model residual vector $\mathbf{e}(t)$ by a transformation matrix \mathbf{W} (Gertler and Singer, 1985)

$$\mathbf{r}(t) = \mathbf{W} \mathbf{e}(t) \quad (15)$$

The matrix \mathbf{W} is designed so that each element of $\mathbf{r}(t)$ is *insensitive* to one particular sensor fault and *sensitive* to other faults. The i th element of $\mathbf{r}(t)$ given that the i th sensor is faulty is represented as

$$r_i(t) = \mathbf{w}_i^T \mathbf{e}(t) = \mathbf{w}_i^T \mathbf{e}^*(t) + \mathbf{w}_i^T \mathbf{b}_j f_j(t) \quad i = 1, 2, \dots, n \quad (16)$$

where \mathbf{w}_i^T is the i th row of matrix $\mathbf{W} \in \mathbb{R}^{n \times m}$. Since $\mathbf{e}^*(t)$ is random noise, one can only design the residual $r_i(t)$ to be insensitive to \mathbf{b}_i . If the actual fault is f_j ($j \neq i$), the residual

$$r_{ij}(t) = \mathbf{w}_i^T \mathbf{e}^*(t) + \mathbf{w}_i^T \mathbf{b}_j f_j(t) \quad (17)$$

we wish to design \mathbf{w}_i such that $r_i(t)$ is not affected by $f_i(t)$ but most affected by $f_j(t)$ ($j \neq i$). This leads to the SRAMS design criterion which is stated as follows:

Choose \mathbf{w}_i such that $r_i(t)$ is insensitive to the i th sensor fault but most sensitive to the others. Mathematically, this is equivalent to

lent to

$$\max_{\mathbf{w}_i} \sum_{j \neq i} \frac{(\mathbf{w}_i^T \mathbf{b}_j)^2}{\|\mathbf{w}_i\|^2 \|\mathbf{b}_j\|^2}$$

subject to

$$\mathbf{w}_i^T \mathbf{b}_i = 0$$

Geometrically, \mathbf{w}_i is chosen to be orthogonal to \mathbf{b}_i while minimizing its angle to other fault directions \mathbf{b}_j ($j \neq i$). This problem can be equivalently stated as follows

$$\max_{j \neq i} \sum_{j=1}^n (\mathbf{w}_i^T \mathbf{b}_j^0)^2 \quad (18)$$

subject to

$$\begin{aligned} \mathbf{w}_i^T \mathbf{b}_i^0 &= 0 \\ \|\mathbf{w}_i\| &= 1 \end{aligned}$$

where

$$\mathbf{b}_j^0 = \frac{\mathbf{b}_j}{\|\mathbf{b}_j\|} \quad j = 1, 2, \dots, n. \quad (19)$$

To satisfy the constraint $\mathbf{w}_i^T \mathbf{b}_i^0 = 0$, the vector \mathbf{w}_i must be chosen as follows

$$\mathbf{w}_i = (\mathbf{I} - \mathbf{b}_i^0 \mathbf{b}_i^{0T}) \mathbf{z}_i \in \mathbf{S}_{\mathbf{w}_i}, \quad \mathbf{z}_i \in \mathbf{R}^m \quad (20)$$

where $\mathbf{S}_{\mathbf{w}_i}$ is the orthogonal complement of \mathbf{b}_i . Therefore, the solution of \mathbf{w}_i is converted to the solution of \mathbf{z}_i . Using a Lagrange multiplier, \mathbf{z}_i can be found by maximizing the following objective

$$\begin{aligned} J &= \max_{\mathbf{z}_i} \sum_{j \neq i} (\mathbf{z}_i^T (\mathbf{I} - \mathbf{b}_i^0 \mathbf{b}_i^{0T}) \mathbf{b}_j^0)^2 + \lambda (1 - \|(\mathbf{I} - \mathbf{b}_i^0 \mathbf{b}_i^{0T}) \mathbf{z}_i\|^2) \\ &= \max_{\mathbf{z}_i} \sum_{j=1}^n (\mathbf{z}_i^T (\mathbf{I} - \mathbf{b}_i^0 \mathbf{b}_i^{0T}) \mathbf{b}_j^0)^2 + \lambda (1 - \|(\mathbf{I} - \mathbf{b}_i^0 \mathbf{b}_i^{0T}) \mathbf{z}_i\|^2) \end{aligned} \quad (21)$$

The above relation holds because $(\mathbf{I} - \mathbf{b}_i^0 \mathbf{b}_i^{0T}) \mathbf{b}_i^0 = \mathbf{0}$. Denoting $[\mathbf{b}_1^0, \dots, \mathbf{b}_n^0] \equiv \mathbf{B}^0$ and

$$(\mathbf{I} - \mathbf{b}_i^0 \mathbf{b}_i^{0T}) [\mathbf{b}_1^0, \dots, \mathbf{b}_n^0] = (\mathbf{I} - \mathbf{b}_i^0 \mathbf{b}_i^{0T}) \mathbf{B}^0 \equiv \mathbf{B}_i^0 \quad (22)$$

which is the projection of \mathbf{B}^0 onto $\mathbf{S}_{\mathbf{w}_i}$, the maximization problem can be rearranged as follows

$$J = \max_{\mathbf{z}_i} \|\mathbf{B}_i^0 \mathbf{z}_i\|^2 + \lambda (1 - \mathbf{z}_i^T (\mathbf{I} - \mathbf{b}_i^0 \mathbf{b}_i^{0T}) \mathbf{z}_i) \quad (23)$$

Differentiating J with respect to \mathbf{z}_i leads to

$$\mathbf{B}_i^0 \mathbf{B}_i^{0T} \mathbf{z}_i = \lambda (\mathbf{I} - \mathbf{b}_i^0 \mathbf{b}_i^{0T}) \mathbf{z}_i \quad (24)$$

Note that

$$\begin{aligned} \mathbf{B}_i^{0T} &= \mathbf{B}^{0T} (\mathbf{I} - \mathbf{b}_i^0 \mathbf{b}_i^{0T}) \\ &= \mathbf{B}^{0T} (\mathbf{I} - \mathbf{b}_i^0 \mathbf{b}_i^{0T})^2 \\ &= \mathbf{B}_i^{0T} (\mathbf{I} - \mathbf{b}_i^0 \mathbf{b}_i^{0T}) \end{aligned} \quad (25)$$

Equation 24 can be rearranged as

$$\mathbf{B}_i^0 \mathbf{B}_i^{0T} (\mathbf{I} - \mathbf{b}_i^0 \mathbf{b}_i^{0T}) \mathbf{z}_i = \lambda (\mathbf{I} - \mathbf{b}_i^0 \mathbf{b}_i^{0T}) \mathbf{z}_i$$

or

$$\mathbf{B}_i^0 \mathbf{B}_i^{0T} \mathbf{w}_i = \lambda \mathbf{w}_i \quad (26)$$

Therefore \mathbf{w}_i is the eigenvector of $\mathbf{B}_i^0 \mathbf{B}_i^{0T}$ that corresponds to the largest eigenvalue (other eigenvalues do not maximize J).

Alternative design methods

In the previous discussions we design one structured residual to be insensitive to only one fault. For instance, for the case of five sensors ($n=5$) with a model of four equations ($m=4$), the structured residual for sensor one will have an incidence vector as $[0 \ 1 \ 1 \ 1 \ 1]$ (Gertler and Singer, 1985, 1990), where “0” means insensitive and “1” means *most* sensitive. However, the SRAMS design method can be extended to having one residual insensitive to several faults while most sensitive to other faults. For example, we can design the incidence vector for the first residual as $[0 \ 1 \ 0 \ 1 \ 1]$, which makes the residual insensitive to both sensor faults 1 and 3. If this type of design is desirable, one must make sure that there are extra degrees of freedom left for maximizing sensitivity to other faults and the isolability conditions are met (Gertler, 1988).

In this subsection we propose a design method for a residual to be insensitive to several faults. Suppose one wishes to design the i th structured residual to be insensitive to a group of sensors with an index set g_i where $i \in g_i$, and most sensitive to the other sensors with an index set \bar{g}_i . For example, for the case of five sensors, $g_i = \{1, 3\}$ and $\bar{g}_i = \{2, 4, 5\}$ represent that the residual should be insensitive to sensor faults 1 and 3 but most sensitive to sensor faults 2, 4 and 5. Then, the corresponding columns of \mathbf{B} are regrouped in \mathbf{B}_{g_i} and $\mathbf{B}_{\bar{g}_i}$ and Eq. 3 can be rewritten as

$$\mathbf{e}(t) = \mathbf{B}\mathbf{x}(t) = [\mathbf{B}_{g_i} \ \mathbf{B}_{\bar{g}_i}] \begin{bmatrix} \mathbf{x}_{g_i}(t) \\ \mathbf{x}_{\bar{g}_i}(t) \end{bmatrix}$$

The i th structured residual ($i \in g_i$) is

$$r_i(t) = \mathbf{w}_i^T \mathbf{e}(t) = \mathbf{w}_i^T \mathbf{B}_{g_i} \mathbf{x}_{g_i}(t) + \mathbf{w}_i^T \mathbf{B}_{\bar{g}_i} \mathbf{x}_{\bar{g}_i}(t)$$

The SRAMS design requires that $r_i(t)$ be insensitive to faults in $\mathbf{x}_{g_i}(t)$ but most sensitive to faults in $\mathbf{x}_{\bar{g}_i}(t)$. Mathematically, \mathbf{w}_i should be chosen to

$$J = \max_{\|\mathbf{w}_i\|=1} \|\mathbf{w}_i^T \mathbf{B}_{\bar{g}_i}\|^2 \quad (27)$$

subject to

$$\mathbf{w}_i^T \mathbf{B}_{g_i} = \mathbf{0} \quad (28)$$

Since \mathbf{B}_{g_i} may have linearly dependent columns, singular value decomposition can be performed on \mathbf{B}_{g_i} ,

$$\mathbf{B}_{g_i} = \mathbf{U}_{g_i} \mathbf{D}_{g_i} \mathbf{V}_{g_i}^T$$

where \mathbf{D}_{g_i} contains only non-zero singular values of \mathbf{B}_{g_i} . Therefore, we choose \mathbf{w}_i in the orthogonal complement of \mathbf{U}_{g_i} to satisfy Eq. 28

$$\mathbf{w}_i = (\mathbf{I} - \mathbf{U}_{g_i} \mathbf{U}_{g_i}^T) \mathbf{z}_i \in S_{w_i} \quad (29)$$

similar to the single sensor fault case. Furthermore, the following objective is maximized

$$\max_{\mathbf{z}_i} \|\mathbf{z}_i^T (\mathbf{I} - \mathbf{U}_{g_i} \mathbf{U}_{g_i}^T) \mathbf{B}^0\|^2 = \max_{\mathbf{z}_i} \|\mathbf{z}_i^T \mathbf{B}_{g_i}^0\|^2 \quad (30)$$

subject to

$$\|(\mathbf{I} - \mathbf{U}_{g_i} \mathbf{U}_{g_i}^T) \mathbf{z}_i\| = 1$$

where

$$\mathbf{B}_{g_i}^0 \equiv (\mathbf{I} - \mathbf{U}_{g_i} \mathbf{U}_{g_i}^T) \mathbf{B}^0 \quad (31)$$

After using a Lagrange multiplier, \mathbf{z}_i is found to be the solution to the following equation

$$\mathbf{B}_{g_i}^0 \mathbf{B}_{g_i}^{0T} \mathbf{z}_i = \lambda (\mathbf{I} - \mathbf{U}_{g_i} \mathbf{U}_{g_i}^T) \mathbf{z}_i \quad (32)$$

Since $\mathbf{B}_{g_i}^{0T} = \mathbf{B}_{g_i}^{0T} (\mathbf{I} - \mathbf{U}_{g_i} \mathbf{U}_{g_i}^T)$ as a result of Eq. 31, we obtain

$$\mathbf{B}_{g_i}^0 \mathbf{B}_{g_i}^{0T} (\mathbf{I} - \mathbf{U}_{g_i} \mathbf{U}_{g_i}^T) \mathbf{z}_i = \lambda (\mathbf{I} - \mathbf{U}_{g_i} \mathbf{U}_{g_i}^T) \mathbf{z}_i$$

or

$$\mathbf{B}_{g_i}^0 \mathbf{B}_{g_i}^{0T} \mathbf{w}_i = \lambda \mathbf{w}_i \quad (33)$$

Therefore, \mathbf{w}_i is simply the eigenvector of $\mathbf{B}_{g_i}^0 \mathbf{B}_{g_i}^{0T}$ associated with the largest eigenvalue.

Comparison to structured residual approach

The conventional structured residual approach (Gertler et al., 1985, 1990) chooses \mathbf{w}_i to be insensitive to one or several faults of interest, but it does not maximize the sensitivity to other faults. In a structured residual design, the selection of \mathbf{w}_i is not unique and somewhat arbitrary, if some residuals are not designed to be insensitive to the maximum number of faults. The arbitrariness in this design leads to a suboptimal solution which does not maximize the potential to isolate faults. With the proposed SRAMS method, we achieve a

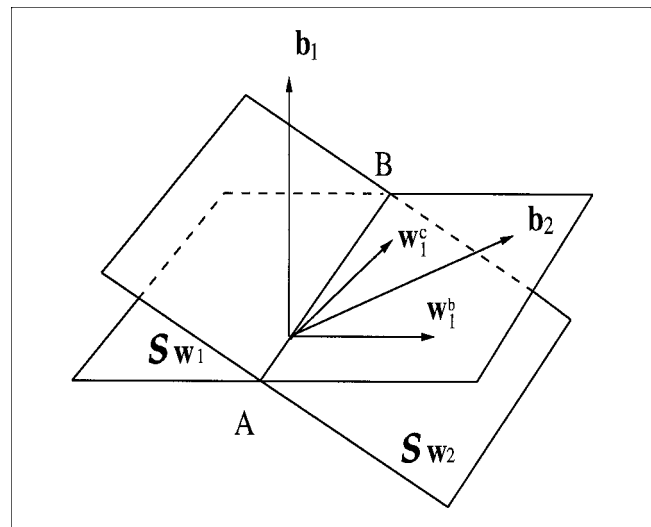


Figure 1. \mathbf{w}_1^b has a smallest angle with \mathbf{b}_2 , however, \mathbf{w}_1^c can be orthogonal to \mathbf{b}_2 .

unique design of \mathbf{w}_i that maximizes the sensitivity to other faults while being insensitive to the faults of interest.

The difference between the SRAMS method and the conventional structured residual method can be further illustrated geometrically. Figure 1 depicts the case of two different sensor faults, \mathbf{b}_1 and \mathbf{b}_2 , in a three-dimensional space. The planes orthogonal to \mathbf{b}_1 and \mathbf{b}_2 are denoted as S_{w1} and S_{w2} , respectively, which share the same line AB . The SRAMS method chooses \mathbf{w}_1^b and S_{w1} plane which has the minimum angle (or most sensitive) to \mathbf{b}_2 . The conventional structured residual approach can choose \mathbf{w}_1^c arbitrarily in the plane S_{w1} , which discounts its sensitivity to \mathbf{b}_2 fault. As the worst case, \mathbf{w}_1^c could be collinear with AB , which is impossible to isolate \mathbf{b}_1 and \mathbf{b}_2 . In a typical design, however, the conventional design chooses somewhere between the worst case (AB line) and the best case (SRAMS design), thus avoiding the worst case by verifying $\mathbf{w}_1^T \mathbf{b}_2 \neq 0$. Nevertheless the conventional approach lacks a systematic design to find the best case.

Fault Identification Indices

In this section, four types of fault identification indices are investigated: (1) EWMA-filtered structured residuals; (2) generalized likelihood ratio; (3) cumulative sum of residuals; (4) cumulative variances. The first three indices are similar in the sense that they are designed to filter high frequency noise by a moving window or a forgetting factor approach. The last index is intended to be particularly sensitive to variance-type of faults. The definition of the identification indices and the determination of the confidence limits for each index are presented next.

Confidence limits for the filtered structured residuals

After a set of structured residuals have been generated, a decision about which sensor fails has to be made. Ideally, each structured residual $r_f(t)$ is supposed to be zero or close to zero when no sensor fails. However, due to modeling er-

rors, measurement noise and other uncertainties, $r_i(t)$ is never equal to zero. Therefore, a confidence limit for each $r_i(t)$, $i = 1, 2, \dots, n$, should be determined using statistical techniques.

With no fault or any sensors in g_i being faulty, based on the SRAMS design, the i th structured residual follows a normal distribution

$$r_i(t) = \mathbf{w}_i^T \mathbf{e}(t) = \mathbf{w}_i^T (\mathbf{e}^*(t) + \mathbf{B}_{g_i} \mathbf{f}_i(t)) \\ = \mathbf{w}_i^T \mathbf{e}^*(t) \sim \mathcal{N}(0, \mathbf{w}_i^T \mathbf{R}_e \mathbf{w}_i) \quad (34)$$

Consequently

$$\frac{r_i^2(t)}{\mathbf{w}_i^T \mathbf{R}_e \mathbf{w}_i} \sim \chi^2(1) \quad (35)$$

Therefore, the confidence limit for $r_i^2(t)$ is

$$\eta_i^\alpha = \mathbf{w}_i^T \mathbf{R}_e \mathbf{w}_i \chi_\alpha^2(1) \quad (36)$$

where α is the level of significance.

When an EWMA filter is applied to the structured residual, the filtered structured residual (FSR) is

$$\bar{r}_i(t) = \gamma \bar{r}_i(t-1) + (1-\gamma) r_i(t) \\ = (1-\gamma) \sum_{k=0}^{\infty} \gamma^k r_i(t-k) \quad (37)$$

If there is no fault, $\bar{r}_i(t)$ also follows normal distribution with $E\{\bar{r}_i(t)\} = E\{r_i(t)\} = 0$ and

$$\text{var}\{\bar{r}_i(t)\} = \frac{1-\gamma}{1+\gamma} \left[1 + 2 \sum_{k=1}^{\infty} \gamma^k \psi_i(k) \right] \text{var}\{r_i(t)\} \quad (38)$$

where

$$\psi_i(k) = \frac{E\{r_i(t) r_i(t-k)\}}{E\{r_i(t)^2\}}$$

is the auto-correlation function. Therefore, the alarming threshold for $\bar{r}_i^2(t)$ is

$$\bar{\eta}_i^\alpha = \frac{1-\gamma}{1+\gamma} \left[1 + 2 \sum_{k=1}^{\infty} \gamma^k \psi_i(k) \right] \mathbf{w}_i^T \mathbf{R}_e \mathbf{w}_i \chi_\alpha^2(1), \\ i = 1, 2, \dots, n \quad (39)$$

If all sensors are normal, the probability

$$P\{\bar{r}_i^2(t) > \bar{\eta}_i^\alpha\} = \alpha$$

If sensor $i \in g_i$ is faulty, by the SRAMS design, $\bar{r}_i^2(t)$ is not affected by the fault. However, the other residuals $\bar{r}_j^2(t)$, $j \notin g_i$ will increase significantly because their sensitivity to sensor $i \in g_i$ is maximized. This will allow us to identify the faulty sensors. We define an identification index based on FSR as

follows

$$I_{FSR}^i(t) = \frac{\bar{r}_i^2(t)}{\bar{\eta}_i^\alpha} \quad (40)$$

Under normal conditions, $I_{FSR}^i(t)$ ($i = 1, 2, \dots, n$) are less than one. If sensor $i \in g_i$ is faulty, $I_{FSR}^i(t)$ will be less than one, but all other $I_{FSR}^j(t)$ ($j \notin g_i$) will be larger than one.

Since there are usually many sensors to be validated, the probability for one or more residuals to exceed the threshold is significant, even though the probability for each index to exceed its threshold is small. For example, assuming that there are 20 independent residuals $\bar{r}_i(t)$, $i = 1, 2, \dots, 20$. The probability for at least one residual to exceed its threshold is (assuming $\alpha = 0.05$)

$$P = 1 - (1 - \alpha)^{20} = 1 - 0.95^{20} = 0.642$$

even though all sensors are normal. Therefore, one should not use the structured residuals for fault detection. Instead, we use the filtered detection index \bar{d} to detect whether there is a sensor fault.

Generalized likelihood ratio test

If the sensor fault incurs significant changes in the mean, such as bias, drift, and complete failure, the generalized likelihood ratio test is usually appropriate to use (Benveniste et al., 1987; Basseville and Nikiforov, 1993). As shown in Eq. 34, if no sensor is faulty, $r_i(t)$ is zero-mean and normally distributed. However, if the j th sensor ($j \in g_i$) becomes faulty at instant t_f

$$r_i(t) = \mathbf{w}_i^T \mathbf{e}^*(t) + \mathbf{w}_i^T \mathbf{b}_j f_j(t)$$

is no longer zero-mean. Assuming the variance is unchanged, we have

$$r_i(t) \sim \begin{cases} \mathcal{N}(0, \mathbf{w}_i^T \mathbf{R}_e \mathbf{w}_i) & \text{if } t < t_f, \\ \mathcal{N}(\mu_{ij}, \mathbf{w}_i^T \mathbf{R}_e \mathbf{w}_i) & \text{if } t \geq t_f. \end{cases}$$

where

$$\mu_{ij} = \mathbf{w}_i^T \mathbf{b}_j f_j(t) \quad (41)$$

To detect the mean change of $r_i(t)$, we define the following GLR function

$$S_{t_f}^i(\mu_{ij}) = \frac{\sum_{k=t_f}^t r_i^2(k) - \sum_{k=t_f}^t (r_i(k) - \mu_{ij})^2}{\mathbf{w}_i^T \mathbf{R}_e \mathbf{w}_i} \quad (42)$$

Differentiating $S_{t_f}^i(\mu_{ij})$ with respect to μ_{ij} produces the optimal estimate of μ_{ij}

$$\hat{\mu}_{ij} = \frac{\sum_{k=t_f}^t r_i(k)}{t - t_f + 1} \quad (43)$$

where the instant t_f can be chosen as the time when the detection index $\bar{d}(t)$ exceeds its limit \bar{d}_α .

With $\hat{\mu}_{ij}$ in Eq. 43, $S_{t_f}^i(\mu_{ij})$ is maximized with

$$S_{t_f}^i(\hat{\mu}_{ij}) = \frac{(t - t_f + 1) \hat{\mu}_{ij}^2}{\mathbf{w}_i^T \mathbf{R}_e \mathbf{w}_i} \quad (44)$$

If sensor $j \in g_i$ is faulty, $\mu_{ij} = 0$ for $i \in g_j$, and $r_i(t) \sim N(0, \mathbf{w}_i^T \mathbf{R}_e \mathbf{w}_i)$. From Eq. 43

$$\hat{\mu}_{ij} \sim N\left(0, \frac{\mathbf{w}_i^T \mathbf{R}_e \mathbf{w}_i}{t - t_f + 1}\right)$$

or

$$S_{t_f}^i(\hat{\mu}_{ij}) = \frac{(t - t_f + 1) \hat{\mu}_{ij}^2}{\mathbf{w}_i^T \mathbf{R}_e \mathbf{w}_i} \sim \chi^2(1), \quad i, j \in g_i \quad (45)$$

Therefore, if sensor $j \in g_i$ is faulty,

$$\begin{cases} S_{t_f}^i(\hat{\mu}_{ij}) \leq \chi_\alpha^2(1) & \text{for } i \in g_i, \\ S_{t_f}^i(\hat{\mu}_{ij}) > \chi_\alpha^2(1) & \text{for } i \notin g_i. \end{cases}$$

From the above analysis, we define an identification index based on GLR as follows

$$I_{GLR}^i(t) = \frac{S_{t_f}^i(\hat{\mu}_{ij})}{\chi^2(1)} \quad (46)$$

Under normal conditions, $I_{GLR}^i(t)$ ($i = 1, 2, \dots, n$) are less than one. If sensor $j \in g_i$ is faulty, $I_{GLR}^i(t)$ will be less than one for $i \in g_j$, but all other $I_{GLR}^i(t)$ ($i \notin g_j$) will be larger than one.

The GLR index can be implemented as a cumulative average or moving average in real time. For the cumulative average implementation, one chooses t_f to be the time a fault is detected, that is, $t_f = \hat{t}_f$. For moving average implementation, one chooses $t_f = \max(t - t_w, \hat{t}_f)$, where t_w is the width of the moving window.

Qsum and Vsum indices

Cumulative sum (Qsum) are often used in statistical process control to make it sensitive to mean changes. In this work, Qsum of the residual $r_i(k)$ is introduced as follows to detect mean changes due to sensor faults

$$Q_{\text{sum}}(t, i) = \sum_{k=t_f}^t r_i(k) \quad (47)$$

The Qsum index is sensitive to mean changes. However, it is difficult to establish a confidence limit for $Q_{\text{sum}}(t, i)$ since it is nonstationary. The only way to find a confidence limit for Qsum is to relate it to GLR. Since

$$Q_{\text{sum}}(t, i) = (t - t_f + 1) \hat{\mu}_{ij} \quad (48)$$

we have the following relation from Eq. 44

$$Q_{\text{sum}}^2(t, i) = (t - t_f + 1) \mathbf{w}_i^T \mathbf{R}_e \mathbf{w}_i S_{t_f}^i(\hat{\mu}_{ij}) \quad (49)$$

Since $S_{t_f}^i(\hat{\mu}_{ij}) \sim \chi_\alpha^2(1)$, the confidence limit for Q_{sum}^2 is $(t - t_f + 1) \mathbf{w}_i^T \mathbf{R}_e \mathbf{w}_i \chi_\alpha^2(1)$. This confidence limit increases linearly with the number of data points. A normalized index for Qsum can be defined as follows

$$I_{Q_{\text{sum}}}^i(t) = \frac{Q_{\text{sum}}^2(t, i)}{(t - t_f + 1) \mathbf{w}_i^T \mathbf{R}_e \mathbf{w}_i \chi_\alpha^2(1)} \quad (50)$$

A value larger than one for this index indicates a faulty situation.

If a sensor incurs a precision degradation fault (that is, mainly variance change), both Qsum and GLR will have difficulty identifying it. For this reason, we propose a cumulative variance (Vsum) index to be sensitive to faults that cause variance to change. The Vsum index is calculated as follows

$$V_{\text{sum}}(t, i) = \sum_{k=t_f}^t (r_i(k) - \hat{\mu}_{ij})^2, \quad i = 1, 2, \dots, n. \quad (51)$$

Under normal conditions, the following ratio follows a Chi-square distribution with $t - t_f$ degree of freedom (Hald, 1952)

$$\frac{V_{\text{sum}}(t, i)}{\mathbf{w}_i^T \mathbf{R}_e \mathbf{w}_i} \sim \chi^2(t - t_f)$$

Therefore, we define a normalized index for Vsum

$$I_{V_{\text{sum}}}^i(t) = \frac{V_{\text{sum}}(t, i)}{\mathbf{w}_i^T \mathbf{R}_e \mathbf{w}_i \chi_\alpha^2(t - t_f)} \quad (52)$$

A value above one for this index indicates an abnormal situation. If sensor $j \in g_i$ is faulty

$$\begin{cases} I_{V_{\text{sum}}}^i(t) \leq 1 & \text{for } i \in g_i, \\ I_{V_{\text{sum}}}^i(t) > 1 & \text{for } i \notin g_i. \end{cases}$$

Note that the Qsum and Vsum indices can also be implemented as a cumulative average or moving average in real time, similar to the case of GLR.

Fault Estimation and Classification

Fault estimation

The best reconstruction method proposed by Dunia et al. (1996) can be used to estimate the sensor fault size after the faulty sensor has been identified. If there is a sensor fault, the model residual $\mathbf{e}(t)$ will increase in magnitude according to Eq. 3. Since the fault direction has been identified, we estimate the fault magnitude $f_i(t)$ in the direction Ξ_i by minimizing

$$J = \|\mathbf{e}^*(t)\|^2 = \|\mathbf{e}(t) - \mathbf{B}\Xi_i f_i(t)\|^2 \quad (53)$$

A least-square solution to this problem leads to

$$\hat{f}_i(t) = (B\Xi_i)^+ e(t) \quad (54)$$

where $(\cdot)^+$ is the Moore-Penrose pseudo inverse.

Distinguishing sensor faults from process changes

Although the ultimate objective of this work is to detect and identify sensor faults, process changes, whether normal or abnormal, can interfere with the sensor validation results and cause fault alarms. Therefore, it is important to isolate sensor faults from process changes.

Typically, process changes can be classified into three categories:

- (i) Unmeasured, normal process disturbances;
- (ii) Slow process degradation which may or may not lead to a process fault; and
- (iii) Abnormal process changes which prohibit the process to function normally.

These process changes can be further divided into two types: additive and multiplicative changes. For example, leakage in a pipeline system is a typical additive fault, a process parameter variation is a typical multiplicative fault. Unmeasured process disturbances can affect the process either as an additive change (such as ventilation) or as a multiplicative change (such as inlet concentration). In principle, both additive and multiplicative changes affect the residuals differently from sensor faults. Therefore, they can be distinguished from sensor faults. To deal with the effect of additive changes $s(t) \in \mathbb{R}^{n_s}$, we can write the model residual and the structured residuals as follows assuming no sensor faults

$$\begin{aligned} x(t) &= x^*(t) + \Xi_s s(t) \\ e(t) &= e^*(t) + B\Xi_s s(t) \\ r_i(t) &= w_i^T e^*(t) + w_i^T B\Xi_s s(t) \quad i = 1, 2, \dots, n \end{aligned} \quad (55)$$

where $\Xi_s \in \mathbb{R}^{m \times n_s}$ is the direction in which the disturbance or fault affects the measurement. As long as Ξ_s is not included in any one of the sensor faults, all the structured residuals are affected by the disturbances or faults. Therefore, based on this analysis, we can distinguish sensor faults from process disturbances or faults.

Another approach to dealing with a process disturbance is to include it in the design of the matrix known process disturbance. The structured residuals $r(t)$ can be designed to be zero-sensitive to this disturbance by choosing w_i orthogonal to Ξ_s and b_i simultaneously.

The case of multiplicative changes typically leads to a change in the process model, that is

$$B_p x(t) \equiv (B + \Delta B) x(t) = e^*(t)$$

where $B_p \equiv B + \Delta B$ is the process matrix which is different

from the model matrix B , and $e^*(t)$ is zero mean Gaussian noise. The structured residuals are still generated based on the model matrix B , that is

$$r_i(t) = w_i^T B x(t) = w_i^T e^*(t) - w_i^T \Delta B x(t)$$

The first term on the righthand side of the above equation is random noise and defines the confidence limit, while the second term is the effect of multiplicative process changes. Since the process parameter change ΔB typically does not coincide with a sensor fault direction, multiplicative process faults can also be distinguished from sensor faults based on the above analysis. In summary, if the fault detection index detects a faulty situation and all structured residuals are affected, it is likely due to a process change.

Case Study: A Boiler Process

In recent years, industrial boiler furnaces are required to be equipped with continuous monitoring systems (CEMS) (EPA, 1991). Traditionally, this requirement is complied with hardware analyzers (Mandel, 1996). Hardware CEMS are typically used in the following manner: (i) the probe is installed near the top of the stack to take samples; (ii) the samples are transported to the analyzing equipment on the ground with a heated cable to maintain the same temperature as they were sampled; and (iii) the CEMS need to be re-calibrated a few times a day with inert gases. Due to these requirements, the hardware CEMS are usually high-cost and prone to malfunctions. Therefore, alternative approaches such as inferential sensors have been developed (Qin et al., 1997). Among the EPA requirements for CEMS, three of them are important: (i) EPA permits the use of software means for air emission monitoring; (ii) the inferential model must have a correlation coefficient better than a specified value, say 80%; and (iii) the CEMS has to be on-line for at least 95% of the time. The last requirement mandates a sensor validation mechanism in the inferential sensor approach. In this section, we demonstrate how the proposed SRAMS approach is applied to (i) detect sensor faults; (ii) identify faulty sensors; (iii) estimate the fault magnitude; and (iv) reconstruct the faulty sensors.

Over 630 data points were collected from an industrial boiler process at a five minute sampling interval. The data were collected during a period of significant change in the boiler throughput so as to cover a wide range of the process behavior. Seven input variables are considered which are listed in Table 1. In the same table the variables' minimum, maximum, and mean values are also listed.

We scale data to zero mean and unit variance and then build a process model using PCA. The number of principal components is determined to be one based on the best reconstruction criterion developed by Qin and Dunia (1998) and the identified process model is as follows

$$B = \begin{bmatrix} -0.1466 & -0.0950 & -0.1198 & -0.1282 & -0.3028 & -0.1012 & 0.9147 \\ -0.1017 & -0.0788 & 0.1813 & 0.8058 & -0.3142 & -0.4481 & -0.0414 \\ 0.0967 & 0.6896 & 0.3149 & -0.2982 & -0.5361 & -0.1660 & -0.1093 \\ -0.1522 & 0.1498 & 0.2087 & -0.2053 & 0.5983 & -0.7062 & 0.1097 \\ -0.7627 & 0.4782 & -0.2731 & 0.1977 & 0.1347 & 0.2403 & -0.0094 \\ -0.4570 & -0.3376 & 0.7684 & -0.1486 & -0.0553 & 0.2473 & -0.0194 \end{bmatrix}$$

Table 1. Process Variables for the Boiler Process

Variable Name	Sensor No.	Minimum	Maximum	Mean	Unit
Air flow	1	215.88	415.74	341.98	Kpb/h
Fuel flow	2	10.480	20.130	16.430	%
Steam flow	3	150.96	300.62	244.12	Kpb/h
Economizer temperature	4	622.66	737.81	699.53	°F
Stack pressure	5	2.020	10.790	7.105	H ₂ O
Wind-box pressure	6	2.690	11.300	7.520	H ₂ O
Feed water flow	7	172.97	308.18	253.58	Kpb/h

We conduct scenarios: (1) a single sensor being faulty; (2) two sensors being simultaneously faulty. In each case, the transformation matrix W , the threshold \bar{d}_α for fault detection

$$W = \begin{bmatrix} -0.0201 & 0.2781 & 0.1678 & 0.2504 & -0.5134 & 0.7535 \\ -0.0239 & -0.1780 & -0.0963 & -0.2277 & -0.4254 & -0.8519 \\ -0.0458 & 0.0238 & -0.0010 & -0.0687 & -0.9407 & -0.3281 \\ 0.0262 & 0.1525 & 0.1394 & 0.2401 & 0.4728 & 0.8219 \\ 0.0317 & 0.1807 & 0.1516 & 0.2172 & 0.4689 & 0.8224 \\ 0.0247 & 0.1961 & 0.1486 & 0.2750 & 0.4504 & 0.8126 \\ 0.0176 & 0.1700 & 0.1308 & 0.2340 & 0.4834 & 0.8157 \end{bmatrix}$$

Therefore, the structured residual vector with seven elements is generated by

$$r(t) = WBx(t) = \begin{bmatrix} 0.0000 & -0.3667 & 0.8772 & -0.0883 & -0.1323 & -0.2642 & -0.0306 \\ 0.7607 & 0.0000 & -0.6456 & -0.0224 & -0.0317 & -0.0539 & -0.0084 \\ 0.8821 & -0.3476 & 0.0000 & -0.0978 & -0.1428 & -0.2645 & -0.0351 \\ -0.7786 & 0.0662 & 0.6209 & 0.0000 & 0.0313 & 0.0532 & 0.0083 \\ -0.7749 & 0.0664 & 0.6259 & 0.0222 & 0.0000 & 0.0534 & 0.0084 \\ -0.7660 & 0.0669 & 0.6382 & 0.0224 & 0.0316 & 0.0000 & 0.0084 \\ -0.7842 & 0.0659 & 0.6135 & 0.0221 & 0.0312 & 0.0530 & 0.0000 \end{bmatrix} x(t)$$

and the confidence limits for FSR, GLR, Qsum, and Vsum are determined off-line before conducting fault detection and identification.

Single sensor fault case

In this scenario, faulty data are simulated by introducing one of the four types of faults: bias, drift, complete failure and precision degradation to one of the sensors. In each case, fault occurrence instant t_f is random. Four identification indices, I_{FSR}^i , I_{GLR}^i , I_{Qsum}^i and I_{Vsum}^i are used to carry out the identification of the faulty sensors. An EWMA filter with a coefficient $\gamma = 0.9$ is applied to generate $\bar{d}(t)$ and FSR for all the four faulty cases. The GLR, Qsum and Vsum indices are calculated based on the unfiltered structured residuals $r(t)$ with a moving window size $t_w = 40$.

Fault Detection Results. We use the following formula to simulate the four types of sensor faults

$$\begin{aligned} \text{bias:} \quad & f_i(t) = b \\ \text{drift:} \quad & f_i(t) = a(t - t_f) \\ \text{complete failure:} \quad & x_i(t) = c \\ \text{precision degradation:} \quad & f_i(t) \sim N(0, \sigma^2) \end{aligned}$$

for $t \geq t_f$. The parameters a , b , c , and σ are constants. Bias, drift, complete failure, and precision degradation are introduced to the air flow, fuel flow, stack pressure, and wind-box pressure, respectively, as shown in Table 2. The fault time, fault size, and the time at which the faults are detected are also listed in the table. The filtered fault detection index for these faulty situations is shown in Figures 2a through 5a. It is seen that in all four cases, the filtered detection index (SPE) is able to detect the fault promptly. The SPE index for the precision degradation fault tends to be noisy due to the nature of the fault.

Fault Identification and Reconstruction Results. Choosing the criterion that the i th structured residual $r_i(t)$ is insensitive to the i th sensor fault but most sensitive to the other sensor faults, we have the following transformation matrix

The fault identification and reconstruction are conducted after the fault has been detected. Figures 2 through 5 show the fault identification and reconstruction results. The sub-plot (c) shows how each FSR responds to the fault in one of the sensors. To make the visualization of the identification results easier, bar charts for the four identification indices are shown in sub-plots (b), (d), (f), and (h). Since these indices are normalized with respect to their confidence limits, any index values above four are clipped, since a value above one already indicates faulty situations. For FSR and GLR indices, the time-averages of the respective indices are shown. The sub-plot (e) for estimated fault size indicates how large the fault is and the type of the faults. The sub-plot (g) is provided to compare the faulty data with reconstructed data.

For the bias fault introduced in sensor 1 (air flow), the FSR, GLR, and Qsum indices shown in Figure 2 are effective in identifying the fault, but the Qsum confidence limit is not reliable. The Vsum index is not effective since the fault is a bias. The estimated fault size indicates that this is a bias fault. The sub-plot (g) for the first sensor shows that the difference between faulty data and reconstructed data is small, indicating the SRAMS method is sensitive to small faults.

For the drift fault introduced in sensor 2 (fuel flow), the FSR, GLR, and Qsum are effective in identifying the fault as

Table 2. Fault Simulation and Detection Results in Single Fault Case

	Bias	Drift	Complete Failure	Precision Degradation
Faulty sensor	Air flow	Fuel flow	Stack pressure	Wind-box pressure
Fault expression	$f_1(t) = 25$	$f_2(t) = 0.01(t - t_f)$	$x_5(t) = 10$	$f_6(t) \sim N(0, 3^2)$
Fault time	222	243	244	254
Detection time	260	359	268	256

shown in Figure 3. The Vsum is not effective. The estimated fault size indicates that this is a drift fault. The plot for the first sensor shows the difference between faulty data and reconstructed data.

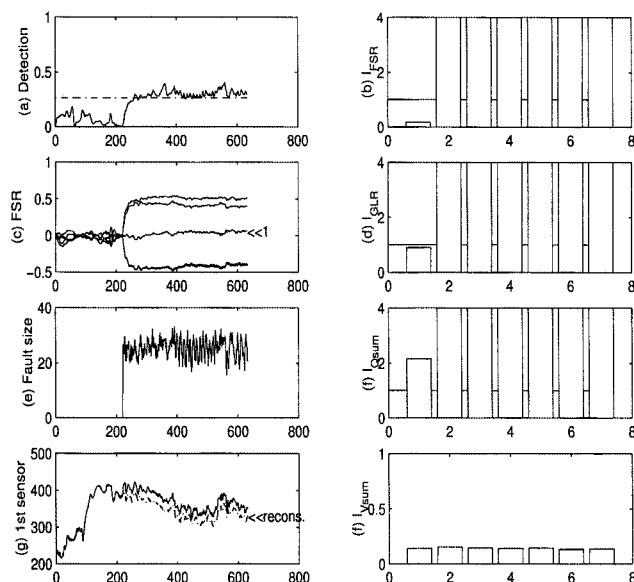


Figure 2. Detection, identification, and reconstruction results for a bias fault in sensor 1 (air flow).

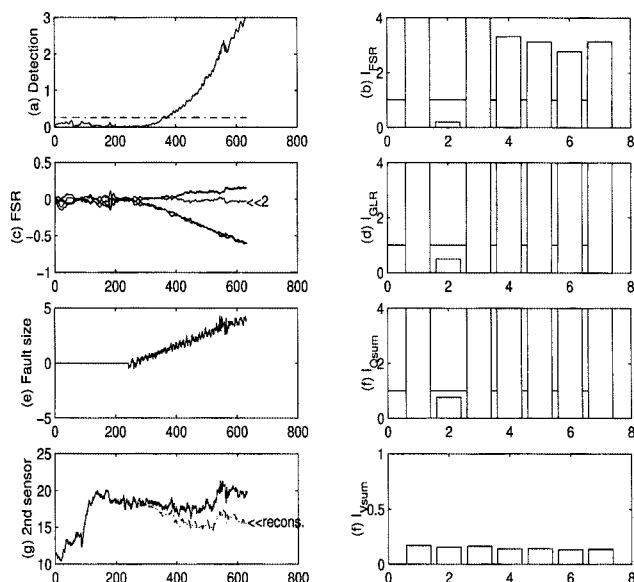


Figure 3. Detection, identification, and reconstruction results for a drift fault in sensor 2 (fuel flow).

Figure 4 shows the identification and reconstruction results for a complete failure in sensor 5 (stack pressure). The FSR, GLR, and Qsum indices are effective in identifying the fault, but the Qsum confidence limit is not reliable. The Vsum index is not effective since the fault is mainly a bias change. The estimated fault size indicates that this is a bias fault.

The case of precision degradation in sensor 6 (wind-box pressure) is shown in Figure 5. Since this fault incurs variance changes only, Vsum is the only effective index. The other three indices fail to identify the faulty sensor. The GLR and FSR indices have smallest values for the sixth sensor, but several other sensors are also below the confidence limits. The fault size estimate indicates clearly that this is the case of precision degradation.

The effectiveness of the fault identification indices is summarized in Table 3. The results show that none of the indices can be sensitive to all types of faults. To identify the faults effectively, these indices should be used jointly. They also provide information about what type of fault has occurred.

Multiple sensor fault case

In this subsection, we consider a scenario to identify two simultaneously faulty sensors from the seven sensors in the boiler process. Faulty data are simulated by introducing any of the four types of faults mentioned above to two sensors at a randomly selected t_f . The parameters a , b , c , and σ^2 used to generate faulty data are listed in Table 4.

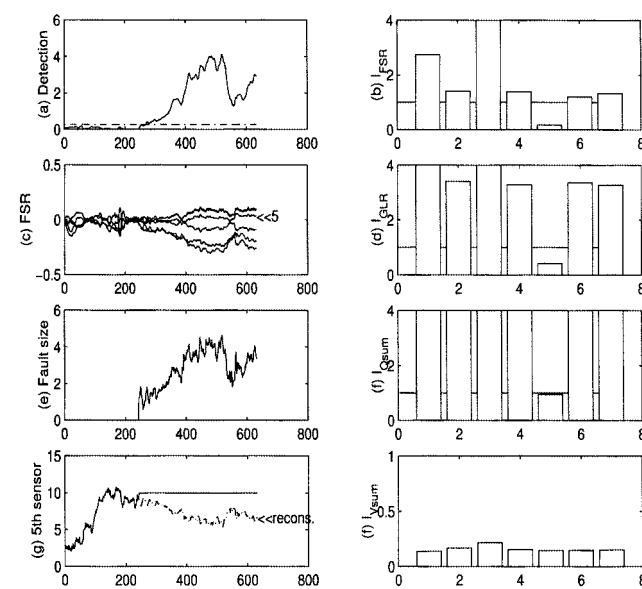


Figure 4. Detection, identification, and reconstruction results for a complete failure in sensor 5 (stack pressure).

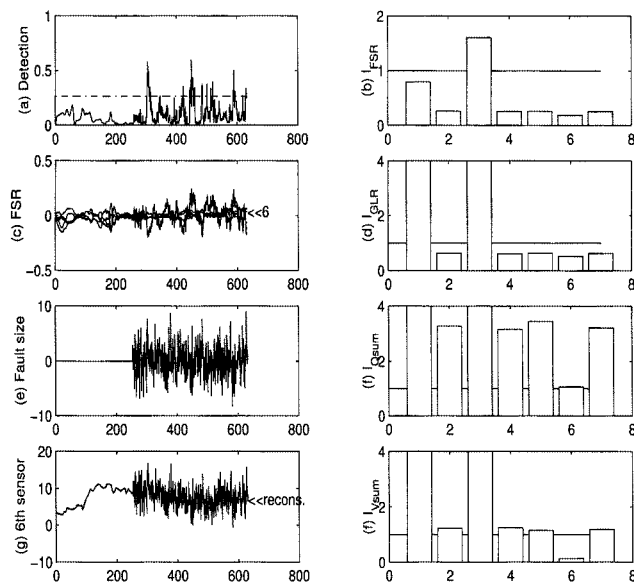


Figure 5. Detection, identification, and reconstruction results for a precision degradation in sensor 6 (wind-box pressure).

To identify two simultaneous faults as well as single sensor faults, we can select the following incidence matrix to generate the seven structured residuals $r_1(t), \dots, r_7(t)$

$$\begin{array}{c|ccccccc} & f_1(t) & f_2(t) & f_3(t) & f_4(t) & f_5(t) & f_6(t) & f_7(t) \\ \hline r_1(t) & 0 & 0 & 0 & 0 & 1 & 1 & 1 \\ r_2(t) & 1 & 0 & 0 & 0 & 0 & 1 & 1 \\ r_3(t) & 1 & 1 & 0 & 0 & 0 & 0 & 1 \\ r_4(t) & 1 & 1 & 1 & 0 & 0 & 0 & 0 \\ r_5(t) & 0 & 1 & 1 & 1 & 0 & 0 & 0 \\ r_6(t) & 0 & 0 & 1 & 1 & 1 & 0 & 0 \\ r_7(t) & 0 & 0 & 0 & 1 & 1 & 1 & 0 \end{array} \quad (56)$$

Since the model matrix B has 6 rows, that is, $m=6$, and g_i four elements, the conditions $w_i^T B = 0$, ($i \in g_i$) and $\|w_i\| = 1$ leave one degree of freedom to maximize Eq. 27.

Accordingly, we obtain the associated transformation matrix

$$W = \begin{bmatrix} 0.0882 & -0.1099 & 0.2505 & -0.9287 & 0.0836 & 0.2189 \\ 0.0973 & -0.2309 & -0.1901 & -0.3586 & 0.7218 & 0.5015 \\ 0.0887 & 0.0182 & 0.3945 & 0.2188 & 0.8820 & 0.1019 \\ 0.0214 & 0.1914 & 0.1868 & 0.2626 & 0.4121 & 0.8302 \\ 0.0143 & -0.0871 & 0.1632 & -0.0888 & 0.5374 & -0.8179 \\ 0.0970 & 0.0654 & 0.6174 & -0.0768 & -0.3481 & 0.6914 \\ 0.1228 & -0.3418 & 0.2427 & -0.8589 & 0.0694 & 0.2582 \end{bmatrix}$$

The resulting seven structured residuals are given as follows

$$r(t) = \begin{bmatrix} 0 & 0 & 0 & 0 & -0.6830 & 0.7288 & -0.0491 \\ -0.7343 & 0 & 0 & 0 & 0 & 0.6759 & 0.0634 \\ -0.7293 & 0.6823 & 0 & 0 & 0 & 0 & 0.0511 \\ -0.7382 & 0.0678 & 0.6711 & 0 & 0 & 0 & 0 \\ 0 & 0.6379 & -0.7599 & 0.1253 & 0 & 0 & 0 \\ 0 & 0 & 0.8050 & -0.2997 & -0.5120 & 0 & 0 \\ 0 & 0 & 0 & -0.2119 & -0.5787 & 0.7875 & 0 \end{bmatrix} x(t) \quad (57)$$

Table 3. Fault Identification Results Using Different Indices for Single Fault Case

	Bias	Drift	Complete Failure	Precision Degradation
FSR	Effective	Effective	Effective	Somewhat effective
GLR	Effective	Effective	Effective	Somewhat effective
Qsum	Effective	Effective	Somewhat effective	Not effective
Vsum	Somewhat effective	Somewhat effective	Not effective	Effective

Table 4. Fault Generation and Detection Results in the Multiple Fault Case

	Bias	Drift	Complete Failure	Precision Degradation
Faulty sensors	Air flow; Fuel flow	Fuel flow; Steam flow	Economizer temperature; Stack pressure	Wind-box pressure; Feedwater flow
Fault expression	$f_1(t) = 25$ $f_2(t) = 6.7$	$f_2(t) = 0.01(t - t_f)$ $f_3(t) = 0.015(t - t_f)$	$x_4(t) = 700$ $x_5(t) = 10$	$f_6(t) \sim N(0, 3.0^2)$ $f_7(t) \sim N(0, 52^2)$
Fault time	250	180	310	220
Detection time	252	315	316	236

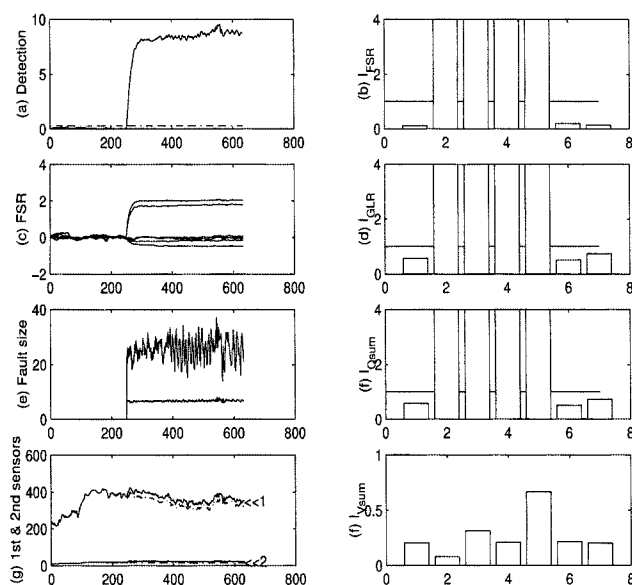


Figure 6. Detection, identification, and reconstruction results for biases in sensors 1 and 2 (air flow and fuel flow).

With only seven structured residuals designed above, we can identify uniquely seven single sensor faults and $(2/7) = 21$ simultaneously double faults. First of all, the single sensor fault case can be easily identified using the incidence matrix given by Eq. 56. Defining $h = r_1 \times r_2 \times r_3 \times r_4 \times r_5 \times r_6 \times r_7$, we have the following identification logic for single sensor faults

If $h = h_1 = 0 \ 1 \ 1 \ 1 \ 0 \ 0 \ 0$, then sensor 1 is faulty
 If $h = h_2 = 0 \ 0 \ 1 \ 1 \ 1 \ 0 \ 0$, then sensor 2 is faulty
 If $h = h_3 = 0 \ 0 \ 0 \ 1 \ 1 \ 1 \ 0$, then sensor 3 is faulty
 \vdots
 If $h = h_7 = 1 \ 1 \ 1 \ 0 \ 0 \ 0 \ 0$, then sensor 7 is faulty

Secondly, for simultaneous double faults, the following identification logic holds

If $h = h_i \vee h_j$, then sensor i and j fail simultaneously

where \vee stands for binary OR. For example, if $h = 0 \ 0 \ 1 \ 1 \ 1 \ 0 \ 0 = h_2 \vee h_3$, then sensors 2 and 3 fail simultaneously.

We have carried all the 21 scenarios, but only four of them are included in this article due to limited space. Fault detection results are shown in Table 4, where fault expression, fault magnitude, fault occurrence time, and the detection time are included. The filtered fault detection index for these four scenarios is shown in Figures 6a through 9a. It can be seen that the filtered detection index (SPE) is able to detect the faults promptly.

The fault identification and reconstruction are conducted after a fault has been detected and the analysis for the results is similar to that for the single sensor fault case. Figures 6 through 9 show the fault identification and reconstruction results. For the bias fault introduced in sensors 1 and 2 (air

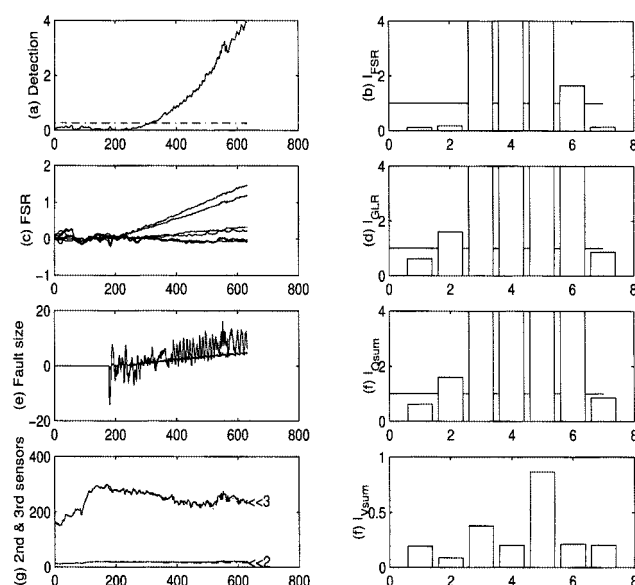


Figure 7. Detection, identification, and reconstruction results for drifts in sensors 2 and 3 (air flow and economizer temperature).

flow and fuel flow) in Figure 6, the FSR and GLR indicate $h = 0 \ 1 \ 1 \ 1 \ 0 \ 0 \ 0$, which is effective in identifying the faults, but the Qsum indices are not reliable and the Vsum indices are not effective. For the drift faults introduced in sensors 2 and 3 (fuel flow and economizer temperature) in Figure 7, the FSR index shows $h = 0 \ 0 \ 1 \ 1 \ 1 \ 0 \ 0$, which is effective in identifying the faults, but the GLR and Qsum indices are not reliable and the Vsum indices are not effective.

Figure 8 shows the identification and reconstruction results for complete failures in sensors 4 and 5 (steam flow and

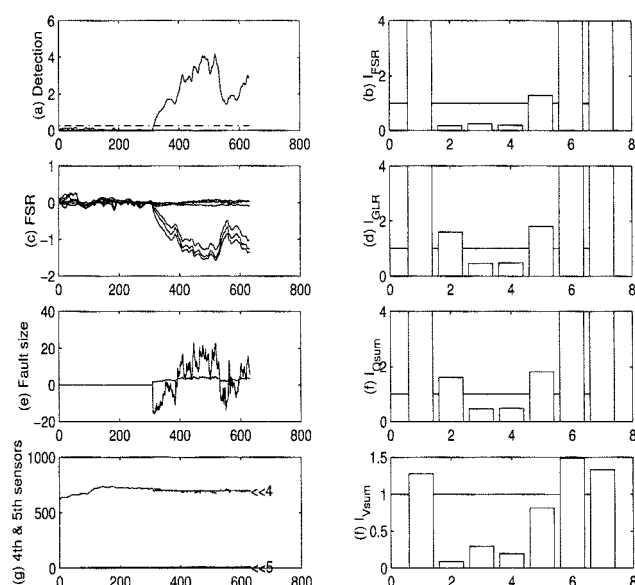


Figure 8. Detection, identification, and reconstruction results for complete failures in sensors 4 and 5 (steam flow and stack flow).

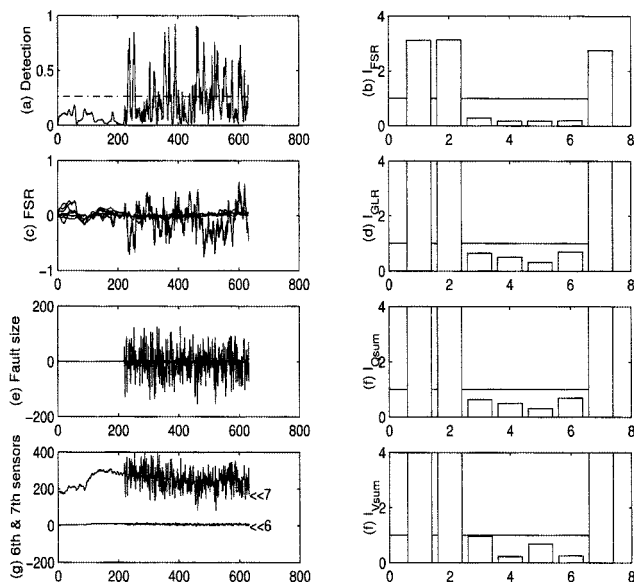


Figure 9. Detection, identification, and reconstruction results for precision degradations in sensors 6 and 7 (wind-box pressure and feedwater flow).

stack pressure). The FSR index is effective in identifying the faults, but the GLR and Qsum indices are not reliable, and the Vsum index is not effective.

The case of precision degradations in sensors 6 and 7 (wind-box pressure and feed water flow) is shown in Figure 9. Since these faults incur variance changes only, Vsum is the only effective index. FSR and GLR are not reliable and Qsum fails to identify the faulty sensors.

Conclusions

A novel sensor fault detection, identification, and reconstruction scheme is proposed based on the concept of structured residuals with maximized sensitivity. The structured residuals are designed such that each of them is unaffected by a subset of sensor faults but maximally sensitive to the others. An EWMA filter is used to pre-process the model residual and structured residuals in order to reduce the effects of transients and the number of false alarms. The confidence limits for both fault detection and identification indices are developed using statistical methods. Four types of sensor faults: bias, drift, complete failure, and precision degradation are considered. Four indices of fault identification, FSR, GLR test, Qsum, and Vsum, are applied. Comparisons of these indices are successfully conducted with different types of faults. Distinguishing sensor faults from process faults and disturbances is also achievable with the proposed method. The proposed scheme is successfully applied to an industrial boiler process with single and double sensor faults without increasing the number of residuals.

While our fault identification method makes one residual insensitive to a group of faults, but most sensitive to the others, alternative methods (Narasimhan and Mah, 1988; Dunia et al., 1996) are available that make one index most sensitive

to one fault. The relationship between these two seemingly complementary strategies deserves further investigation. Future work also includes the generalization of the method to fully dynamic processes and the conditions for identifiability and detectability with respect to noise and fault magnitudes.

Acknowledgments

Financial support for this project from Aspen Technology and National Science Foundation through CTS-9814340 is gratefully acknowledged. The authors wish to thank Dr. John Guiver of Aspen Technology for insightful discussions for the development of the method.

Literature Cited

- Albuquerque, J. S., and L. T. Biegler, "Data Reconciliation and Gross-Error Detection for Dynamic Systems," *AIChE J.*, **42**, 2841 (1996).
- Basseville, M., and I. V. Nikiforov, *Detection of Abrupt Changes—Theory and Applications*, Prentice-Hall, Englewood Cliffs, NJ (1993).
- Benveniste, A., M. Basseville, and G. Moustakides, "The Asymptotic Local Approach to Change Detection and Model Validation," *IEEE Trans. Auto. Cont.*, **32**, 583 (1987).
- Crowe, C. M., "Data Reconciliation—Progress and Challenges," *J. Proc. Cont.*, **6**, 89 (1996).
- Crowe, C. M., A. Hrymak, and Y. A. Garcia Campos, "Reconciliation of Process Flow Rates by Matrix Projection. i. The Linear Case," *AIChE J.*, **29**, 881 (1983).
- Deckert, J. C., M. N. Desai, J. J. Deyst, and A. S. Willsky, "F-8 DFBW Sensor Failure Identification Using Analytical Redundancy," *IEEE Trans. Auto. Cont.*, **22**, 796 (1977).
- Dunia, R., J. Qin, T. F. Edgar, and T. J. McAvoy, "Sensor Fault Identification and Reconstruction Using Principal Component Analysis," *Proc. 13th IFAC World Congress*, **Volume N**, 259 (1996).
- EPA, "40CFR Part-75—Continuous Emission Monitoring," *Federal Register* (1991).
- Fantoni, P., and A. Mazzola, "Applications of Autoassociative Neural Networks for Signal Validation in Accident Management," *Proc. the IAEA Specialist Meeting on Advanced Information Methods and Artificial Intelligence in Nuclear Power Plant Control Rooms* (1994).
- Gertler, J., and D. Singer, "Augmented Models for Statistical Fault Isolation in Complex Dynamic Systems," *Proc. Amer. Control Conf.*, 317 (1985).
- Gertler, J., and D. Singer, "A New Structural Framework for Parity Equation Based Failure Detection and Isolation," *Automatica*, **26**, 381 (1990).
- Gertler, J., "Survey of Model-Based Failure Detection and Isolation in Complex Plants," *IEEE Cont. Sys. Mag.*, **12**, 3 (1988).
- Gertler, J., W. Li, Y. Huang, and T. McAvoy, "Isolation-Enhanced Principal Component Analysis," *AIChE J.*, **45**, 323 (1999).
- Hald, A., *Statistical Theory with Engineering Applications*, Wiley (1952).
- Jackson, J. E., and G. Mudholkar, "Control Procedures for Residuals Associated with Principal Component Analysis," *Technometrics*, **21**, 341 (1979).
- Karjala, T. W., and D. M. Himmelblau, "Dynamic Rectification of Data via Recurrent Neural Nets and the Extended Kalman Filter," *AIChE J.*, **42**, 2225 (1996).
- Keeler, J., and B. Ferguson, "Commercial Applications of Soft Sensors: The Virtual On-Line Analyzer and the Software Cem," *Proc. IFPAC Conf.* (1996).
- Kramer, M., "Nonlinear Principal Component Analysis Using Autoassociative Neural Networks," *AIChE J.*, **37**, 233 (1991).
- Liebman, M. J., T. F. Edgar, and L. S. Lasdon, "Efficient Data Reconciliation and Estimation for Dynamic Processes Using Nonlinear Programming Techniques," *Comput. Chem. Eng.*, **16**, 963 (1992).
- Mah, R. S. H., G. M. Stanley, and D. Downing, "Reconciliation and Rectification of Process Flow and Inventory Data," *Ind. Eng. Chem. Proc. Des. Dev.*, **15**, 175 (1976).
- Mandel, S., "Continuous Emission Monitoring Systems: An Overview," *Control Eng.*, 47 (Apr. 1996).

- Miller, P., R. E. Swanson, and C. F. Heckler, "Contribution Plots: The Missing Link in Multivariate Quality Control," *Proc. Fall Conf. of the ASQC and ASA* (1993).
- Narasimhan, S., and R. S. H. Mah, "Generalized Likelihood Ratios for Gross Error Identification in Dynamic Processes," *AIChE J.*, **34**, 1321 (1988).
- Qin, S. J., H. Yue, and R. Dunia, "Self-Validating Inferential Sensors with Application to Air Emission Monitoring," *Ind. Eng. Chem. Res.*, **36**, 1675 (1997).
- Qin, S. J., and R. Dunia, "Determining the Number of Principal Components for Best Reconstruction," *Proc. IFAC DYCOPS'98*, Greece (1998).
- Rollins, D. K., and J. F. Davis, "Unbiased Estimation of Gross Errors in Process Measurements," *AIChE J.*, **38**, 563 (1992).
- Romagnoli, J. A., and G. Stephanopoulos, "Rectification of Process Measurement Data in the Presence of Gross Errors," *Chem. Eng. Sci.*, **36**, 1849 (1981).
- Stanley, G. M., and R. S. H. Mah, "Estimation of Flows and Temperatures in Process Networks," *AIChE J.*, **23**, 642 (1977).
- Stanley, G. M., and R. S. H. Mah, "Observability and Redundancy in Process Data Estimation," *Chem. Eng. Sci.*, **36**, 259 (1981).
- Tong, H., and C. M. Crowe, "Detection of Gross Errors in Data Reconciliation by Principal Component Analysis," *AIChE J.*, **41**, 1712 (1995).

Manuscript received Dec. 21, 1998, and revision received May 26, 1999.

Correction

In the article titled "Cyclic Scheduling of Continuous Parallel-Process Units with Decaying Performance" by Vipul Jain and Ignacio E. Grossmann (pp. 1623–1636, July 1998) the following corrections are made:

- The fourth parameter b_{il} in Table 2 (p. 1632) should read as:

Parameter	Furnace l	Feed i						
		A	B	C	D	E	F	G
b_{il} (1/d)	1	0.10	0.20	0.10	0.20	0.23	0.34	0.20
	2	0.2	0.1	0.2	0.25	0.29	0.27	0.30
	3	0.3	0.2	0.3	0.27	0.28	0.29	0.25
	4	0.2	0.2	0.15	0.25	0.29	0.22	0.28

- The second line of the fourth heading of Table 3 (p. 1633) should read "Total Vars.," not "Cont. Vars."
- On the third line of the last paragraph in the second column of p. 1625 and Eq. 2 of p. 1626 "parameter P_i ..." should be replaced by "parameter P_{il} ..."
- On p. 1627, Eq. 12, "0.0001" should be replaced by "0.01."
- On p. 1631, the second line of the third paragraph in the first column "... , 26 continuous variables ..." should be replaced by "... 26 variables ..."; the second line of the fourth paragraph in the second column "... , 233 continuous variables ..." should be replaced by "... , 233 variables ..."